$Zr_{1-x}M_xWMoO_{8-x/2}$ 和 $Zr_{1-x}M_xW_2O_{8-x/2}$ 固溶体的晶胞参数与晶格畸变的关系

郭富丽　马　辉　杨晓晶　邓学彬　赵新华*

(北京师范大学化学学院和分析测试中心,北京　100875)

摘要：合成了 $Zr_{1-x}M_xWMoO_{8-x/2}$(M=Er,Tm,Yb,Sc,In,Ga,Al)和 $Zr_{1-x}M_xW_2O_{8-x/2}$(M=Eu,Er,Yb,Sc,In,Ga,Al)2 个系列的固溶体,前者具有 β-ZrW_2O_8 结构类型 (简称 β 相); 后者具有 α-ZrW_2O_8 结构类型 (简称 α 相)。建立了相和相的晶胞参数与 M^{3+}离子浓度的 Vegard 方程,测定了上述固溶体的固溶度。讨论了 M^{3+}离子的化学性质与 Vegard 斜率 S_V 的关系。分析了 α 相的 S_α^A 与 β 相的 S_β^A 的关系；揭示了 α-$Zr_{1-x}M_xW_2O_{8-x/2}$ 晶格中 2[WO_4]四面体对的取向有序程度对晶格畸变的贡献。提出上述固溶体的晶胞参数随溶质浓度增加而减小,主要是由于氧空位缺陷相互作用的结果。

关键词：固溶体；固溶度；负热膨胀性质；Vegard 斜率
中图分类号：O614.41+2；O614.61+3；O614.61+2　　**文献标识码**：A　　**文章编号**：1001-4861(2011)10-2061-05

Effect of Lattice Parameters of $Zr_{1-x}M_xWMoO_{8-x/2}$ and $Zr_{1-x}M_xW_2O_{8-x/2}$ Solid Solutions on Lattice Distortion

GUO Fu-Li　MA Hui　YANG Xiao-Jing　DENG Xue-Bin　ZHAO Xin-Hua*

(*College of Chemistry, Analysis and Test Center, Beijing Normal University, Beijing* 100875, *China*)

Abstract: The $Zr_{1-x}M_xWMoO_{8-x/2}$ (M=Er, Tm, Yb, Sc, In, Ga, Al) and $Zr_{1-x}M_xW_2O_{8-x/2}$ (M=Sc, In, Ga, Al) solid solutions were synthesized. Their XRD patterns show typical structure of β- and α- ZrW_2O_8, respectively. The lattice parameters $\alpha's$ for both series of solid solutions are linear functions of the M^{3+} concentration^M within the limited solubility, and could be described by Vegard equations with the slope of S_α^M or S_β^M dependent of the difference in ionic radius and the electro-negativity of the M^{3+} ion. However, S_α^M of α-$Zr_{1-x}M_xW_2O_{8-x/2}$ appears to be also associated with the partial orientation of 2[WO_4] pair. In addition, the contraction of the lattice parameters observed for both series of the solid solutions are possibly caused primarily by the oxygen vacancy defect.

Key words: solid solution; solid solubility; negative thermal expansion; vegard slope

0　Introduction

$ZrW_{2-y}Mo_yO_8$ with cubic ZrW_2O_8 (c-ZrW_2O_8) type structure [1] is well-known as a class of materials of considerable isotropic thermal contraction over a wide temperature range [2]. Recently, it has been reported that the thermal stability and electric conductivity are improved in the equivalent substituted $Zr_{1-x}M_xW_{2-y}Mo_yO_8$

(M: Hf^{4+}, Sn^{4+}, Ti^{4+}) [3] and aliovalent substituted $Zr_{1-x}M_xW_2O_{8-x/2}$ (M: Sc^{3+}, In^{3+}, Y^{3+}, Lu^{3+}, Yb^{3+}, Er^{3+}, Eu^{3+}) solid solutions, and the phase transition temperature (T_c) is adjusted even the M^{3+} substitution is as low as only a few percents [4].

Among $ZrW_{2-y}Mo_yO_8$ thermal contraction solid solutions, $ZrWMoO_8$ with c-ZrW_2O_8 type structure should be another favorable matrix besides ZrW_2O_8.

Because the T_c of $ZrWMoO_8$ is as low as 270 K [5] and its thermal stability is elevated up to 1 073 K[2b]. Therefore, we are interested in synthesizing the $Zr_{1-x}M_xWMoO_{8-x/2}$ (M: trivalent metal ions) solid solutions and comparing their properties with $Zr_{1-x}M_xW_2O_{8-x/2}$.

The limited solid solubility of some $Zr_{1-x}Ln_xW_2O_{8-x/2}$ (Ln^{3+}=Eu, Er, Yb) solid solutions was reported in the previous work [2d]. In this work, supplemental solid solutions $Zr_{1-x}M_xW_2O_{8-x/2}$ (M^{3+}=Sc, In, Ga, Al) and another series of solid solutions $Zr_{1-x}M_xWMoO_{8-x/2}$ (M^{3+}=Er, Tm, Yb, Sc, In, Ga, Al) were synthesized and characterized. It is found that the lattice parameters αs for these solid solutions are a linear function of M^{3+} concentration x^M and can be described by Vegard equations with slopes $S_α^M$ and $S_β^M$, which are dependent of the nature of the M^{3+} ions (therefore marked a superscript M by the item), especially the ionic radius and their electro-negativity.

1　Experimental

$Zr_{1-x}M_xWMoO_{8-x/2}$ (M=Er, Tm, Yb, Sc, In, Ga, Al) and $Zr_{1-x}M_xW_2O_{8-x/2}$ (M=Sc, In, Ga, Al) solid solutions were prepared from commercially available $ZrOCl_2 \cdot 8H_2O$, $(NH_4)_{10}W_{12}O_{41} \cdot 5H_2O$, $(NH_4)_6Mo_7O_{24} \cdot 4H_2O$, Al$(NO_3)_3 \cdot 9H_2O$ and M_2O_3 (M=Er, Tm, Yb, Sc, In, Ga) of AR reagents by the previously described procedures[2d]. Briefly, according to the stoichiometric requirement, M_2O_3 was dissolved in a nitric acid (for Al, Al$(NO_3)_3$ was used) and added to $ZrOCl_2/(NH_4)_6Mo_7O_{24}$ or $ZrOCl_2$ aqueous solution for preparation of $Zr_{1-x}M_xWMoO_{8-x/2}$ or $Zr_{1-x}M_xW_2O_{8-x/2}$, respectively. The solution was dropped under stirring into a $(NH_4)_{10}W_{12}O_{41} \cdot 5H_2O$ solution to give a white co-precipitate, and then dried at ~373 K. After triturated, the obtained powder was annealed at 873 K for 3 h and used as the precursor.

The precursors were annealed at different temperatures using a Pt crucible and then followed by quenching in atmosphere. For $Zr_{1-x}M_xWMoO_{8-x/2}$ (M=Er, Tm, Yb, Sc, In, Ga, Al) the precursor pellets were annealed at 1 253 K for 1 h; for $Zr_{1-x}M_xW_2O_{8-x/2}$ (M=Sc, In)and $Zr_{1-x}M_xW_2O_{8-x/2}$ (M=Al, Ga), first at 1 473 K for 2 h or 1 453 K for 1 h, respectively, followed by annealing at 1 433 K for 3 h.

X-ray diffraction (XRD) patterns were collected by the procedure described previously [2d]. The lattice parameter was calculated with the Unitcell program [6] by indexing the XRD reflections using SiO_2 (PDF # 33-1161) as the internal standard.

2　Results and discussion

The XRD patterns of $Zr_{1-x}M_xWMoO_{8-x/2}$ (M=Er, Tm, Yb, Sc, In, Ga, Al) solid solutions displayed in Fig.1 (a) can be well indexed to the structure model of cubic $ZrWMoO_8$ (Space Group: $Pa\bar{3}$[7], hereafter denoted as $β$-$Zr_{1-x}M_xWMoO_{8-x/2}$ solid solutions). The similar XRD patterns obtained for $Zr_{1-x}M_xW_2O_{8-x/2}$ (M=Sc, In, Ga, Al) solutions are shown in Fig.1 (b), but the substitution of the Mo by the second W ion in these cases leads to occurrence of a 310 diffraction of super-structure, which is related to an ordered structure characteristic for $α$-ZrW_2O_8 type (Space Group: $P2_13$[1]; denoted as $α$-$Zr_{1-x}M_xW_2O_{8-x/2}$ solid solutions).

As shown in Fig.2, the lattice parameter $α$ for all the solid solutions varies with the substitutions M^{3+} and the substituted concentration of M^{3+}, x^M. The exhibited

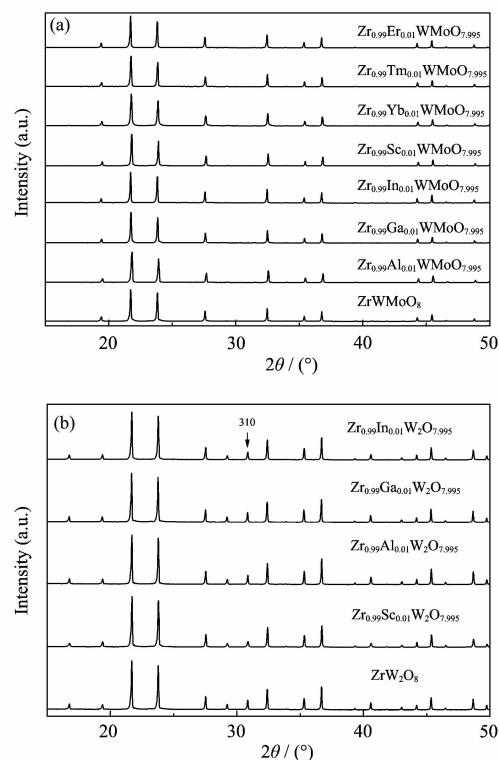Fig.1　XRD patterns of (a) $ZrWMoO_8$ and $Zr_{0.99}M_{0.01}WMoO_{7.995}$; (b) ZrW_2O_8 and $Zr_{0.99}M_{0.01}W_2O_{7.995}$ solid solutions at room temperature
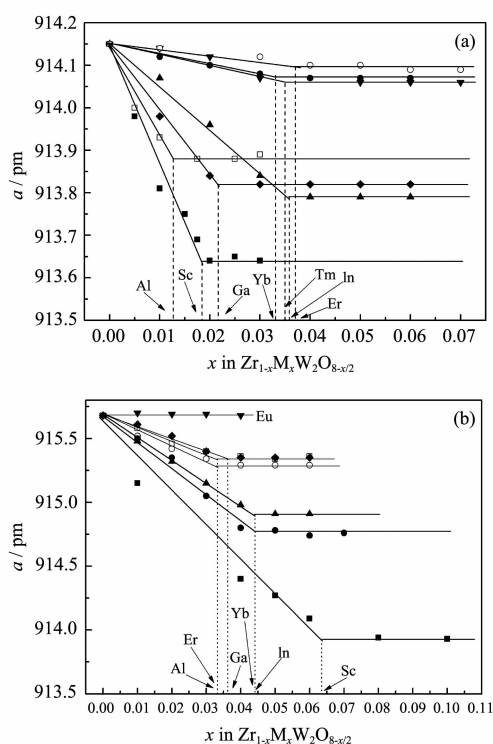
Data of α-Zr$_{1-x}$M$_x$W$_2$O$_{8-x/2}$(M=Eu, Er, Yb) refer to Ref.2d

Fig.2　Dependence of lattice parameter a on M^{3+}
concentration x^M for solid solutions (a)
β-Zr$_{1-x}$M$_x$WMoO$_{8-x/2}$ (M=Er○, Tm▼, Yb●,
Sc■, In▲, Ga◆, Al□) and (b) α-Zr$_{1-x}$M$_x$W$_2$O$_{8-x/2}$
(M=Eu▼, Er○, Yb●, Sc■, In▲, Ga◆, Al□)
at room temperature

dependence of lattice parameter on x^M can be described by Vegard equation (1) when $x_M < x_{th}{}^M$, a "threshold", above which lattice parameter approaches to a constant [2d], corresponding to the saturated solubility of the solid solutions (Table 1):

$$\begin{cases} a_\beta{}^M = a_\beta{}^O + S_\beta{}^M \cdot x^M \\ a_\alpha{}^M = a_\alpha{}^O + S_\alpha{}^M \cdot x^M \end{cases} \quad (x^M \leqslant x_{th}{}^M) \tag{1}$$

Where the lattice parameters for β-Zr$_{1-x}$M$_x$WMoO$_{8-x/2}$ and α-Zr$_{1-x}$M$_x$W$_2$O$_{8-x/2}$ solid solutions are noted as $a_\beta{}^M$ and

$a_\alpha{}^M$, respectively. They are dependent of substitution M^{3+}. $a_\beta{}^O$ (914.15 pm) and $a_\alpha{}^O$ (915.68 pm) are lattice parameters of ZrWMoO$_8$ and α-ZrW$_2$O$_8$ at room temperature. The slopes $S_\beta{}^M$ and $S_\alpha{}^M$ are characteristic parameters for the dependence of lattice distortion on the M^{3+} ionic radii involved in the β-Zr$_{1-x}$M$_x$WMoO$_{8-x/2}$ and α-Zr$_{1-x}$M$_x$W$_2$O$_{8-x/2}$ solid solutions, respectively.

A close inspection of Fig.2 (ref Table.1) reveals that the slopes $S_\beta{}^M$ and $S_\alpha{}^M$ of Vegard equations (1) appear to be a function of the difference in radius, Δr, and the charge change, ΔZ, of the ions involved M^{3+} and can be described by equations (2):

$$\begin{cases} S_\beta{}^M = C_{\beta 1}\Delta r - C_{\beta 2}\Delta Z \\ S_\alpha{}^M = C_{\alpha 1}\Delta r - C_{\alpha 2}\Delta Z \end{cases} \tag{2}$$

where $\Delta r = r(M^{3+}) - r(Zr^{4+})$, $\Delta Z = Z(M^{3+}) - Z(Zr^{4+}) = -1$, $C_{\beta 1}$, $C_{\beta 2}$ and $C_{\alpha 1}$, $C_{\alpha 1}$ are constants related to the relative size and charge difference of with respect to Zr^{4+}.

Fig.3 demonstrates the linear dependence of $S_\beta{}^M$ or $S_\alpha{}^M$ on Δr. It indicates that the Vegard slope is not only dependent on the difference of ionic radii Δr, but is also affected by the electronegativity difference between the substitution and substituted cations even as expatiated by Lubarda for alloy[9]. Based on the argument, $S_\beta{}^M$ or $S_\alpha{}^M$ of the investigated solid solutions are divided into two groups denoted as $S_\beta{}^A$ (M ≡ A=Al, Ga, In) and $S_\beta{}^R$ (M ≡ R=Er^{3+}, Tm^{3+}, Yb^{3+}, Sc^{3+}) with constants $C_{\beta 1}{}^A$, $S_{\beta 2}{}^A$ and $C_{\beta 1}{}^R$, $C_{\beta 2}{}^R$, respectively, according to the closeness in electronegativity. The analogous correlation is also valid for $S_\alpha{}^M$ which is divided into $S_\alpha{}^A$ and $S_\alpha{}^R$ with constants $C_{\alpha 1}{}^A$, $C_{\alpha 2}{}^A$ and $C_{\alpha 1}{}^R$, $C_{\alpha 2}{}^R$.

It is interesting that the values of $C_{v1}{}^R$ are larger than that of $C_{v1}{}^A$ (v is a sign of α or β) in α-Zr$_{1-x}$M$_x$W$_2$O$_{8-x/2}$ or β-Zr$_{1-x}$M$_x$WMoO$_{8-x/2}$ as shown in Fig.3. This phenomenon seems to be correlated to the fact that the

Table 1　Solid solubilitys $x_{th}{}^M$ and Vegard Slopes $S_\beta{}^M$ and $S_\alpha{}^M$ for β-Zr$_{1-x}$M$_x$WMoO$_{8-x/2}$ and α-Zr$_{1-x}$M$_x$W$_2$O$_{8-x/2}$ solid solutions

M^{3+}	Eu	Er	Tm	Yb	Sc	In	Ga	Al
$r(M^{3+})^*$ / pm	94.7	89.0	88.0	86.8	74.5	80.0	62.0	53.5
$x_{th}{}^M$ (β-phase)	/	0.037	0.035	0.033	0.018	0.036	0.021	0.015
$S_\beta{}^M$ / pm	/	−1.0	−2.6	−2.5	−21.6	−10.4	−15.5	−19.0
$x_{th}{}^M$ (α-phase)	0.016 [2d]	0.033 [2d]	/	0.044 [2d]	0.063	0.044	0.036	0.033
$S_\alpha{}^M$ / pm	0.7	−10.3	/	−16.5	−27.1	−21.2	−9.3	−9.6

*Shannon radius refers to ref[8].
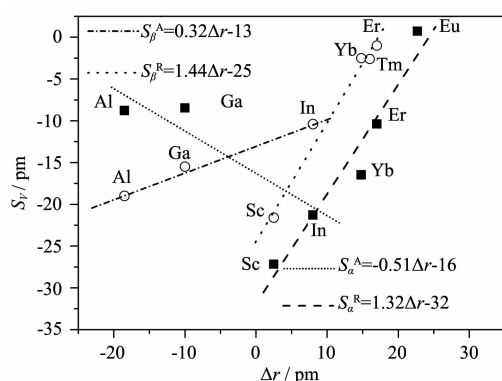
Data of α-Zr$_{1-x}$M$_x$W$_2$O$_{8-x/2}$ (M=Eu, Er, Yb) refer to Ref.2d

Fig.3　Dependence of S_v (the subscript v is α or β) on Δr in β-Zr$_{1-x}$M$_x$WMoO$_{8-x/2}$(M=Er, Tm, Yb, Sc, In, Ga and Al, legend as ○), and α-Zr$_{1-x}$M$_x$W$_2$O$_{8-x/2}$ (M=Eu, Er, Yb, Sc, In, Ga and Al, legend as ■)

electronegativity difference of the elements in the R group is larger than that in the A group with respect to that of O element. In other words, the ionicity is greater between M^{3+} and O^{2-} ion, the lattice distortion owing to the difference of the ionic radius (Δr) is larger.

However, it is noticeable that the contrary sign of $C_{\alpha 1}^A$ and $C_{\beta 1}^A$ in Fig.3 is related to the different matrixes (ordered α-ZrW$_2$O$_8$ and disordered β-ZrWMoO$_8$). The different properties in the two kinds of matrixes will be discussed in the last section.

When Δr=0, C_{v2}^A or C_{v2}^R (v is a sign of α or β) in α-Zr$_{1-x}$M$_x$W$_2$O$_{8-x/2}$ or β-Zr$_{1-x}$M$_x$WMoO$_{8-x/2}$, which are the intercepts on the Vegard slope axis in Fig.3, reflects the effect of the introduction of the aliovalent substitution on the defect of M$_{Zr}$ in the lattice. The effect is that a half amount of oxygen vacancy defects □$_O^{··}$

with double positive charge is introduced in the lattice to maintain the neutrality of the crystal, and the lattice volume is reduced because of the association of the oxygen vacancy defects[10]. As shown in Fig.3, it is the evidence for $C_{v2}^R > C_{v2}^A$ that the interaction of oxygen vacancy in the solid solution substituted by the M^{3+} in R group is stronger than that of the M^{3+} in A group. The association of the oxygen vacancy dominates the contraction of the lattice volume although some radii of M^{3+} are larger than that of Zr^{4+}.

It is reasonable to suggest that the contrary trend of the Vegard slope S_β^A from S_α^A in Fig.3 might be

caused by the additional lattice distortion $\Delta a_{\beta'-\alpha}^O=a_\alpha^O-a_{\beta'}^O$ upon conversion of β-ZrW$_2$O$_8$ to α-ZrW$_2$O$_8$ as well as associated with the change of the parameter ω_T^M in orientational order degree of 2[WO$_4$] tetrahedral pair in α-ZrW$_2$O$_8$ defined as[2d,4b]:

$$\omega_T^M = \sqrt{\frac{[(I_{310}/I_{210})_{Zr_{1-x}M_xW_2O_{8-y}}]_T}{[(I_{310}/I_{210})_{ZrW_2O_8}]_{298\ K}}} \tag{3}$$

Where, ω_T^M is the order degree parameter of 2 [WO$_4$] tetrahedral pair orientation in α-ZrW$_2$O$_8$ structure; I_{hkl} represents the integrate intensity of hkl diffraction.

The ω_T^M is deduced from equation (3) by determining the relative XRD intensity dependent of concentration x^M of the solute and the dependence of $\omega_{298\ K}^M$ on x^M is shown in Fig.4, where $\omega_{298\ K}^M$ linearly related to the concentration^M of M^{3+} in solid solution describes as equation (4):

$$\omega_{298\ K}^M = 1 - C^M x^M \tag{4}$$

The slope C^M can be understood as a structural parameter associated with substitution defect M$_{Zr}$. This defect is thought to be surrounded by disordered tetrahedral pair 2[WO$_4$] to form a local cluster. The total volume of cluster decreases with increasing the ionic radius. Hence, the slope i.e., C^M will be different and inversely proportional to the difference in radii of the ions $\Delta r=r$(M^{3+})$-r$(Zr^{4+}). The orientational order degree parameter ω_{298K}^M is dependent of the species and decreases with increasing the concentration x^M of substitution defects[4b].

Therefore, the Vegard equation (1) for α-Zr$_{1-x}$M$_x$W$_2$O$_{8-x/2}$ solid solutions can be derived from that
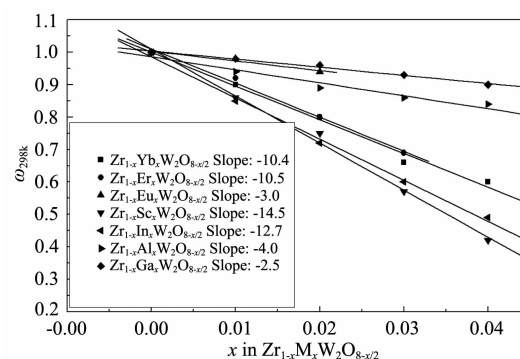
Data of α-Zr$_{1-x}$M$_x$W$_2$O$_{8-x/2}$(M=Er, Yb) refer to Ref.2d

Fig.4　Relative order parameter ($\omega_{298\ K}^M$) as a function of the concentration of M^{3+} in Zr$_{1-x}$M$_x$W$_2$O$_{8-x/2}$

of β-$Zr_{1-x}M_xW_2O_{8-x/2}$ by including the contribution from the lattice increment $\Delta a_{\beta'-\alpha}{}^O$ and orientational order parameter $\omega_{298\ K}{}^M$ induced by different substitution defect M_{Zr}, i.e,

$$a_\alpha{}^M = a_\beta{}^M + \omega_{298\ K}{}^M \Delta a_{\beta'-\alpha}{}^O$$
$$= a_\beta{}^O + S_\beta{}^M x^M + (1 - C^M x^M) \Delta a_{\beta'-\alpha}{}^O$$
$$= a_\alpha{}^O + (S_\beta{}^M - C^M \Delta a_{\beta'-\alpha}{}^O)\, x^M \qquad (5)$$

Where subscript β' denotes β-$Zr_{1-x}M_xW_2O_{8-x/2}$; $\Delta a_{\beta'-\alpha}{}^O$ is 0.82 pm.

Comparing equations (5) with (1) the relationship between $S_\alpha{}^M$ and $S_\beta{}^M$ presents as:

$$S_\alpha{}^M = S_\beta{}^M - C^M \Delta a_{\beta'-\alpha}{}^O \qquad (6)$$

Consequently the lattice distortion of α-$Zr_{1-x}M_xW_2O_{8-x/2}$ solid solution not only results from the different relative size and charge change between M^{3+} and Zr^{4+} ions but also from the orientational order degree change of the tetrahedral pair 2[WO_4]. Equation (6) also can interpret the opposite sign of $C_{\alpha1}{}^A$ against $C_{\beta1}{}^A$ in Fig.3 that the additional contribution $C^M \Delta a_{\beta'-\alpha}{}^O$ of $S_\alpha{}^A$ enhances the lattice distortion of α-$Zr_{1-x}M_xW_2O_{8-x/2}$ than $S_{\beta'}{}^A$ of β-$Zr_{1-x}M_xW_2O_{8-x/2}$, especially the minus slope of $S_\alpha{}^{In}$ results from the larger slope of the dependence of $\omega_{298\ K}{}^{In}$ on x^{In} for α-$Zr_{1-x}In_xW_2O_{8-x/2}$ than that of α-$Zr_{1-x}M_xW_2O_{8-x/2}$ (Ga and Al) solid solutions.

3　Conclusions

Two series solid solutions of β-$Zr_{1-x}M_xWMoO_{8-x/2}$ (M=Er, Tm, Yb, Sc, In, Ga, Al) and α-$Zr_{1-x}M_xW_2O_{8-x/2}$ (M=Sc, In, Ga, Al) were synthesized. The former has the β-ZrW_2O_8 structure with disordered orientation of 2[WO_4] pair, while the latter has the α-ZrW_2O_8 structure with certain ordered 2 [WO_4] pair orientation. For both series of solid solutions, the decrease in lattice parameter (a) with the increasing concentration of the substitutions can be expressed by Vegard equations; and the limited solid solubility of the solid solutions is determined by the threshold of the dependent concentrations. The slopes $S_\alpha{}^M$ and $S_\beta{}^M$ of Vegards equations are specific parameter characteristic for the dependence of lattice distortion on the M^{3+} ion. There is a linear dependence on the difference of ionic radii among the elements in the same group of the periodic table of elements. The lattice distortion is proportional

to the ionicity between M^{3+} and O^{2-} for β-$Zr_{1-x}M_xWMoO_{8-x/2}$ and α-$Zr_{1-x}M_xW_2O_{8-x/2}$. The orientational order degree also enhances the lattice distortion of α-$Zr_{1-x}M_xW_2O_{8-x/2}$ additionally. The minus Vegard slopes $S_\alpha{}^M$ and $S_\beta{}^M$ despite the positive C_{v1} (v denotes α or β) and Δr prove that the association of the oxygen vacancy dominates the contraction of the lattice parameters.

References:

[1] (a) Mary T A, Evans J S O, Vogt T, et al. *Science*, **1996**,**272**: 90-92

(b) Evans J S O, Mary T A, Vogt T, et al. *Chem. Mater.*, **1996**, **8**:2809-2823

[2] (a) Closmann C, Sleight A W. *J. Solid State Chem.*, **1998**, **139**:424-426

(b) Huang L, Xiao Q G, Ma H, et al. *Eur. J. Inorg. Chem.*, **2005**,**2005**:4521-4526

(c) Zhao R Q, Yang X J, Wang H L, et al. *J. Solid State Chem.*, **2007**,**180**:3160-3165

(d) Li H H, Han J S, Ma H, et al. *J. Solid State Chem.*, **2007**, **180**:852-857

[3] (a) Meyer C D, Bouree F, Evans J S O, et al. *J. Mater. Chem.*, **2004**,**14**:2988-2994

(b) Buysser K D, Driessche I V, Putte B V, et al. *J. Solid State Chem.*, **2007**,**180**:2310-2315

(c) Buysser K D, Driessche I V, Putte B V, et al. *Inorg. Chem.*, **2008**,**47**:736-41

(d) Yamamura Y, Masago K, Kato M, et al. *J. Phys. Chem. B*, **2007**,**111**:10118-10122

[4] (a) Nakajima N, Yamamura Y, Tsuji T. *Solid State Commun.*, **2003**,**128**:193-196

(b) Yamamura Y, Nakajima N, Tsuji T, et al. *Phys. Rev. B*, **2004**,**70**:104107-1-104107-6

(c) Li H H, Xia H T, Jing X P, et al. *Solid State Sci.*, **2008**, **10**:1037-1041

(d) Li H H, Xia H T, Jing X P, et al. *Solid State Commun.*, **2007**,**142**:434-436

(e) Yamamura Y, Kato M, Tsuji T. *Thermochim Acta*, **2005**, **431**:24-28

[5] Evans J S O, Hanson P A, Ibberson R M, et al. *J. Am. Chem. Soc.*, **2000**,**122**:8694-8699

[6] Holland T J B, Redfern S A T, Mineral. *Mag.*, **1997**,**61**:65-77

[7] Lind C, Wilkinson A P, Hu Z B, et al. *Chem. Mater.*, **1998**, **10**:2335-2337

[8] Shannon R D. *Acta Cryst.*, **1976**,A32:751-767

[9] Lubarda V A. *Mech. Mater.*, **2003**,**35**:53-68

[10] Kim D J. *J. Am. Ceram. Soc.*, **1989**,**72**:1415-1421